



**Citrullination of histone H3 drives IL-6 production by bone marrow mesenchymal stem cells in MGUS and multiple myeloma** OPEN

G McNee, K L Eales, W Wei, D S Williams, A Barkhuizen, D B Bartlett, S Essex, S Anandram, A Filer, P A H Moss, G Pratt, S Basu, C C Davies, D A Tennant

**Cite this article as:** G McNee, K L Eales, W Wei, D S Williams, A Barkhuizen, D B Bartlett, S Essex, S Anandram, A Filer, P A H Moss, G Pratt, S Basu, C C Davies, D A Tennant, Citrullination of histone H3 drives IL-6 production by bone marrow mesenchymal stem cells in MGUS and multiple myeloma, *Leukemia* accepted article preview 11 July 2016; doi: [10.1038/leu.2016.187](https://doi.org/10.1038/leu.2016.187).

This is a PDF file of an unedited peer-reviewed manuscript that has been accepted for publication. NPG are providing this early version of the manuscript as a service to our customers. The manuscript will undergo copyediting, typesetting and a proof review before it is published in its final form. Please note that during the production process errors may be discovered which could affect the content, and all legal disclaimers apply.



This work is licensed under a Creative Commons Attribution 4.0 International License. The images or other third party material in this article are included in the article's Creative Commons license, unless indicated otherwise in the credit line; if the material is not included under the Creative Commons license, users will need to obtain permission from the license holder to reproduce the material. To view a copy of this license, visit <http://creativecommons.org/licenses/by/4.0/>

Received 9 May 2016; revised 24 June 2016; accepted 1 July 2016; Accepted article preview online 11 July 2016

**Citrullination of histone H3 drives IL-6 production by bone marrow mesenchymal stem cells in MGUS and multiple myeloma**

Gavin McNee<sup>1</sup>, Katherine L Eales<sup>1</sup>, Wenbin Wei<sup>2</sup>, Deborah S Williams<sup>2</sup>, Angelique Barkhuizen<sup>3</sup>, David B Bartlett<sup>2</sup>, Sarah Essex<sup>2</sup>, Seetharam Anandram<sup>3</sup>, Andrew Filer<sup>4</sup>, Paul AH Moss<sup>4</sup>, Guy Pratt<sup>2,5</sup>, Supratik Basu<sup>3,6</sup>, Clare C Davies<sup>2,6</sup> and Daniel A Tennant<sup>1</sup>

<sup>1</sup>Institute of Metabolism and Systems Research, College of Medical and Dental Sciences, University of Birmingham, Birmingham. UK

<sup>2</sup>Institute of Cancer and Genomic Sciences, College of Medical and Dental Sciences, University of Birmingham, Birmingham. UK

<sup>3</sup>Department of Haematology, Royal Wolverhampton NHS Trust, Wolverhampton. UK

<sup>4</sup>Institute of Immunology and Immunotherapy, College of Medical and Dental Sciences, University of Birmingham, Birmingham. UK

<sup>5</sup>Department of Haematology, University Hospitals Birmingham NHS Trust, Birmingham. UK

<sup>6</sup>These authors contributed equally to this study

Correspondence should be addressed to:

Daniel A Tennant

Institute of Metabolism and Systems Research,

College of Medical and Dental Sciences,

University of Birmingham,

Birmingham. B15 2TT UK.

Email: [d.tennant@bham.ac.uk](mailto:d.tennant@bham.ac.uk)

Tel: +44 121 414 8651

**Conflict of Interest**

The authors declare no conflicts of interest

**Running title**

Histone H3 citrullination in MGUS and myeloma

Accepted manuscript

**Abstract**

Multiple myeloma (MM), an incurable plasma cell malignancy, requires localisation within the bone marrow. This microenvironment facilitates crucial interactions between the cancer cells and stromal cell types that permit the tumour to survival and proliferate. There is increasing evidence that the bone marrow mesenchymal stem cell (BMMSC) is stably altered in patients with MM – a phenotype also postulated to exist in patients with monoclonal gammopathy of undetermined significance (MGUS) a benign condition that precedes MM. In this study, we describe a mechanism by which increased expression of peptidyl arginine deiminase 2 (PADI2) by BMMSCs in patients with MGUS and MM directly alters malignant plasma cell phenotype. We identify PADI2 as one of the most highly upregulated transcripts in BMMSCs from both MGUS and MM patients, and that through its enzymatic deimination of histone H3 arginine 26, PADI2 activity directly induces the upregulation of interleukin-6 (IL-6) expression. This leads to the acquisition of resistance to the chemotherapeutic agent, bortezomib, by malignant plasma cells. We therefore describe a novel mechanism by which BMMSC dysfunction in patients with MGUS and MM directly leads to pro-malignancy signalling through the citrullination of histone H3R26.

**Introduction**

Multiple myeloma (MM) is a malignant disease of plasma cells within the bone marrow that, despite improving survival, remains incurable meaning an urgent requirement for novel therapies. One characteristic feature of MM is that a pre-malignant condition known as monoclonal gammopathy of undetermined significance (MGUS) can be present for many years prior to development of overt disease(1). No specific genetic alterations have yet been identified that distinguish patients with MGUS from those with MM, suggesting that another factor, such as transformation of the microenvironment are likely drivers of progression(2, 3). Malignant plasma cells have an absolute requirement for localisation within the bone marrow niche, which leads to a characteristic feature of MM: the relative rarity of disease metastasis to sites outside the marrow microenvironment. This suggests that, in common with most malignancies, stromal support of cancer cell survival in MM is important for maintaining and even driving disease(4-6).

Key cellular components of both the normal and transformed bone marrow niche are the bone marrow mesenchymal stromal cells (BMMSCs). There is now significant evidence to suggest that BMMSCs from patients with MM(7-11) and MGUS(7) are phenotypically different from those derived from healthy patients. Indeed they have not only been shown to exhibit a stably altered transcriptional profile(7), but may also contain a number of genetic lesions(12). The phenotypic changes resulting from this altered transcriptome appear to permit increased stromal support of the malignant plasma cell, and decreased osteoblastic differentiated function (bone mineralisation)(7-11). The former is through both physical (i.e. cell-cell) interactions, and secretion of a number of paracrine factors that support malignant plasma cell survival, proliferation migration and chemoresistance(5, 6, 13). Although a number of signaling pathways have been implicated in the differentiation of BMMSCs there remains a lack of clarity as to their role.

A number of cytokines and chemokines have been shown to be involved in the crosstalk between the bone marrow stroma and malignant plasma cells, including interleukin-6 (IL-6)(14), C-X-C motif chemokine 12 (CXCL12, also known as Stromal-Derived Factor 1 [SDF1])(15), Vascular Endothelial Growth Factor (VEGF)(16), fibroblast growth factor (FGF)(17), tumour necrosis factor  $\alpha$  (TNF $\alpha$ )(18), interleukin-1 $\beta$  (IL-1 $\beta$ )(18) and cMET (also known as Hepatocyte Growth Factor/Scatter Factor (HGF/SF)(19). IL-6 secretion by the cells of bone marrow microenvironment, especially the BMMSC population(7, 9, 11), has been shown to play a role in malignant plasma cell phenotype through increasing resistance to cell death stimuli and driving proliferation(20), as well as downregulating differentiation markers, such as CD38 and CD138(21). It is therefore now clear that through both physical association and paracrine interactions, signaling between BMMSCs and myeloma cells underlie the requirement of myeloma cells for BM localization.

One defining feature of BMMSCs isolated from patient bone marrows is that they retain a transcriptomic profile despite being in culture(7-9, 11, 21). This suggests that they sustain this transcriptome through a stable genetic and/or epigenetic profile. Interestingly, little is known about the epigenetic status of BMMSCs in healthy individuals or of those from MGUS or MM patients. A post-translational modification in which there is increasing interest in both cancer and inflammation is the citrullination of peptidyl arginine, which can occur on many different protein species, including histones(22). These reactions are performed by the calcium-dependent peptidyl arginine deiminase (PADI) family of enzymes of which there are five members (PADI1, 2, 3, 4 and 6) with tissue-specific expression patterns(23-25). PADI2 is ubiquitously expressed, and in many tissues has been reported as the major family member providing peptidyl arginine deiminase activity(26). Importantly, both PADI2 and PADI4 have been shown to be able to alter gene transcription through the citrullination of residues in the histone tails(27-29): a modification that may be physiologically irreversible due to the lack of any known peptidylcitrulline imidating enzyme. This modification is

therefore a good candidate for the creation of a long-term change in the cellular transcriptome, as noted in the BMMSCs of MM patients.

As MM is effectively incurable, and is now accepted to almost always arise from MGUS(1), the phenotype of cells contributing to this benign condition may provide important clues as to factors determining progression to MM. We show here that BMMSCs from patients with both MGUS and MM exhibit a significant shift in their transcriptome compared to those from healthy individuals. In addition, we demonstrate that one of the most upregulated transcripts in BM-MSCs from MGUS and MM, peptidyl arginine deiminase 2 (PADI2) is responsible for mediating increased IL-6 expression from these cells through the deimination of arginine residue 26 of histone H3 (H3R26) to form citrulline (H3R26cit). This increased IL-6 production is sufficient to drive resistance of malignant plasma cells to bortezomib (BTM), a highly clinically relevant anti-myeloma drug. We therefore demonstrate a novel mechanism for BM microenvironment-induced acquisition of drug resistance in MM and importantly, that this phenotype is already present in patients with the apparently benign MGUS.

## Methods

### Patient sample collection, BMMSC isolation and cell culture

Patients with MM and MGUS were recruited from specialist clinics at The Royal Wolverhampton Hospitals NHS Trust and Heart of England NHS Trust, UK. The study received approval from the local ethics committees at South Birmingham, Birmingham East, North, and Solihull, and informed written consent was obtained in accordance with the Declaration of Helsinki in all cases. For patients with MGUS/MM, BM aspirates from the iliac crest were diluted in MACS buffer for removal of the CD138<sup>+</sup> cells using anti-CD138<sup>+</sup> antibody-linked magnetic beads (Miltenyi Biotech, UK), before the remaining cellular fraction was diluted in complete medium, and BMMSCs allowed to adhere to tissue culture plates. Control BMMSCs for the transcriptomic study were obtained by flushing out a section of rib

from patients undergoing thoracotomies with RPMI1640. Around 80% of the patients recruited to this control group had a primary lung tumour: none had bone marrow involvement or had received chemotherapy. Patient number and characteristics for the transcriptomic study are shown in Supplementary Table 1, while those of the BMMSCs used in all other studies are shown in Supplementary Table 2. For the other studies, 'healthy' BMMSCs were isolated from patients undergoing hip surgery, with informed written consent obtained and samples collected through the University of Birmingham Research Tissue Bank (HTA license 12358, REC reference 09/H1010/75). Bone marrow aspirates from the femoral head were diluted in RPMI and the BMMSCs in the non-fatty layer allowed to adhere to tissue culture plates. BMMSCs and the HS5 human bone marrow fibroblast cell line (ATCC CRL11882, LGC Standards, UK, purchased December 2013, tested for mycoplasma every 3 months by PCR) were cultured in RPMI (Sigma, UK) with 10% FBS (Hyclone, UK) at 37°C in a humidified incubator with 5% CO<sub>2</sub>. BMMSCs were allowed to adhere and proliferate to approximately 80% confluence before harvesting. Wild-type or active site mutant PADI2 (C647S), each with N-terminal FLAG tag, were expressed through transient transfection of the cDNAs within the pcDNA3 vector (or empty vector control) using jetPEI (Polyplus transfection, France) for 24 hours before analysis. Where shown, the pan-PADI inhibitor Cl-Amidine (200 µM, Cayman Chemical, USA) was used for 48 or 72 hours. siRNA against PADI2 at 20 nM (Oligo 1: AGCCTTGACTCATTTGGAA, and Oligo 4: AAGCGAATCACCATCAACA) or PADI4 (GCGAAGACCTGCAGGACAT) were transfected using TransIT-TKO (Mirus Bio, USA) and assayed at the timepoint shown.

### **Transcriptomic and Real-time PCR analyses**

At passage 3, mRNA from BMMSCs (Supplementary Table 1) was extracted using the RNeasy mini kit (Qiagen, Germany). mRNA was prepared and hybridized to Affymetrix HuEx-1\_0-st-v2 exon arrays (Affymetrix, USA) as per manufacturer's instructions. Gene level analysis of the Affymetrix exon array was performed using Affymetrix Expression Console with the default settings of "Extended: RMA-Sketch" and Affymetrix annotation

na32. Differentially expressed genes were identified using the limma package(30) with cut-off values of  $p < 0.001$  and absolute fold change  $> 1.5$ . Heatmaps were generated using dChip (<http://www.dchip.org/>) with the default settings. Full dataset is available in the Gene Expression Omnibus repository with accession number GSE80608. For Taqman analyses, RNA was isolated using the RNeasy kit before reverse transcription (AMV reverse transcription kit, Promega, UK). Taqman real-time PCR was performed on an ABI7500; using primer/probe mixes (Supplementary Table 3, Life Technologies, UK). Cycle threshold was automatically determined by ABI7500 software and expression levels were normalized to ACTB and calculated relative to control. All transcript data are presented as median-centred box and whisker (10-90<sup>th</sup> percentile) plots.

#### **Detection of apoptosis by flow cytometry**

Primary BMMSCs from MGUS patients that showed high or low PADI2 protein levels (Supplementary Table 2) were seeded at  $5 \times 10^5$  cells 24 hours before  $10^6$  JJN3 cells were added to a TransWell insert (Costar), 24 hours prior to treatment with 10nM bortezomib. After a further 24 hours, JJN3 cell apoptosis was assessed by Annexin V/propidium iodide staining as per manufacturer's instructions (Life Technologies, UK) and flow cytometry (LSRII; BD Biosciences). The resulting data were gated and quantified (Flow Jo v.7.6.5) and presented after subtraction of background apoptosis of untreated, monocultured JJN3 cells. Where shown, BMMSCs were treated with Cl-Amidine (200  $\mu$ M, 16 hours), which was removed before washing and subsequent incubation with JJN3 cells (within the TransWell insert). Experiments were performed three times and expression analysed in triplicate; data presented as mean  $\pm$  s.e.m.

#### **Measurement of IL6**

HS-5 cell culture supernatants were harvested after treatment with either Cl-Amidine or siRNA and centrifuged to remove dead cells. Supernatants were analysed using an IL-6 detection kit as per manufacturer's instructions (eBioscience). Experiments were performed three times in triplicate; data are presented as mean  $\pm$  s.d. IL-6 from BM plasma was

detected using a multiplex bead analysis approach (Affymetrix, USA). Measurements were performed as per manufacturer's instructions. Briefly, plasma samples, diluted with an equal volume of phosphate-buffered saline, pH7.4, were incubated with monoclonal antibody-coated capture beads for 1 hour at 20°C. Washed beads were further incubated with biotin-labelled polyclonal anti-human cytokine antibody for 30 minutes, streptavidin-phycoerythrin for 30 minutes and analysed on a Luminex 100 bioanalyser (Luminex) and converted to absolute concentrations using standard curves. Data are presented as median-centred box and whisker (10-90<sup>th</sup> percentile) plots.

### **Chromatin Immunoprecipitation**

Chromatin immunoprecipitation was performed as previously described(31). Briefly, HS5 fibroblasts were crosslinked with 1% formaldehyde before neutralisation with 0.125 M glycine. After lysis (10 mM Tris-HCl, pH8.0, 10 mM NaCl, 0.2% NP40, 10 mM sodium butyrate, 50 µg/mL phenylmethylsulfonyl fluoride [PMSF] and 1 µg/mL leupeptin), nuclei were purified, lysed (50 mM Tris-HCl, pH8.1, 10 mM EDTA, 1% SDS, 10 mM sodium butyrate, 50 µg/mL PMSF and 1µg/mL leupeptin) and diluted in immunoprecipitation (IP) buffer (20 mM Tris-HCl, 150 mM NaCl, 2 mM EDTA, 1% Triton X-100, 0.01% SDS, 10 mM sodium butyrate, 50 µg/mL PMSF and 1 µg/mL leupeptin). DNA was sheared to 300-1000 bp, and diluted further in IP buffer. After pre-clearing (normal rabbit IgG), chromatin was co-immunoprecipitated with anti-histone H3 trimethyl K4 (Abcam, ab8580) or anti-histone H3 cit26 (Abcam; ab19847, lot GR146412-1). After washing and elution of protein-DNA complexes from the beads (100 mM NaHCO<sub>3</sub>, 1% SDS), cross-links were reversed by heating, and treated with proteinase K. DNA was purified; primers used to quantify DNA are shown in Supplementary Table 4. Experiments were performed three times and PCR performed in triplicate; data presented as mean ± s.e.m.

### **Western blotting**

Samples were harvested, washed in PBS and after pelleting, lysed directly in lysis buffer (10 mM HEPES/KOH pH7.4, 10 mM KCl, 0.05% NP-40, 1 mM sodium orthovanadate). After

centrifugation of the lysate, the supernatant containing the cytoplasmic components was retained, and the pelleted nuclei were washed with lysis buffer before extraction of the nucleoplasmic protein fraction in low salt lysis buffer (10 mM TRIS/HCl pH7.4, 0.2 mM MgCl<sub>2</sub>). After blocking, membranes were probed with antibodies against actin (AC-40; Sigma, UK), R26cit (ab19847; Abcam, UK), R2,8,17cit (ab5103; Abcam, UK), PADI2 (ab19847; Abcam, UK) or PADI4 (ab128086; Abcam, UK), followed by the appropriate HRP-linked secondary antibody (Cell Signalling, NEB, UK), and visualised using ECL Prime (GE Healthcare).

### Statistics

Sample size for patient studies could not be pre-determined due to lack of similar data on healthy and MGUS populations. No samples were excluded from analyses presented. Error bars are shown for all data presented. All statistics were performed using GraphPad Prism v.6.07. In order to compare different patient groups without assumptions of data distribution, non-parametric tests were used (Mann-Whitney and Kruskal Wallis) with Dunn's post-test comparisons where appropriate. Where statistical tests were used on data from cell culture experiments, student's 2-tailed t-tests with Welch's correction were used to avoid assumptions of variance between groups.

### Results

There is strong evidence to suggest that BMMSCs from patients with MM show a transformed phenotype: supporting malignant plasma cell survival, proliferation, and evasion of chemotherapy-mediated cell death(7-11). The BMMSC phenotype in MGUS patients is less-well characterised(7). We therefore performed a transcriptomic analysis of mRNA extracted from BMMSCs cultured from controls, MGUS and MM patients. BMMSCs isolated from patients with both MGUS and MM show markedly different gene expression profiles compared to the controls (Figure 1, cut-offs used,  $p < 0.001$ , fold change 2.0), consistent with the previous report(7). Although a large number of transcripts were found to be differentially

expressed between controls and MGUS (91) or MM (117; cut-off  $p < 0.001$ , fold change of  $> 2.0$ ; Supplementary Tables 5 and 6), none were found to vary between MGUS and MM using the same statistical cut-offs, and only 32 if these were relaxed (cut-off of  $p < 0.01$ , fold change of  $> 1.3$ ; Supplementary Table 7). Pathway analysis of differentially expressed genes between disease and control groups demonstrated that the most prominent enriched signalling pathway was WNT ( $p = 0.00012$  and  $0.00002$  for MM vs control and MGUS vs control, respectively; Supplementary Tables 8 and 9 and Supplementary Figure 1a), which has been previously implicated in the pathogenesis of MM(32-34). In addition, within the top five upregulated transcripts in MGUS and MM was a member of the PADI family of enzymes, PADI2 (Figure 2a), which was up-regulated over 5-fold in both MGUS and MM patient BMMSCs. Importantly, two other functionally related transcripts were also in the top five; filaggrin, a well-described target of PADI2 (Figure 2b), and SLC14A1, which encodes the urea transporter required for excretion of ammonium produced through PADI2 activity (Figure 2c, Supplementary Figure 1b). Interestingly, we recently published evidence that urea concentrations are significantly increased in the bone marrow plasma of patients with both MGUS and MM, consistent with significantly increased cellular production of ammonium, perhaps through PADI2 activity, in the bone marrow niche(35).

To confirm the increased expression of PADI2 in BMMSCs in MGUS and MM, we assessed both mRNA and protein expression in BMMSCs isolated from an independent cohort of healthy individuals, MGUS and MM patients (Supplementary Table 2). We found that mRNA expression of PADI2 was relatively low in BMMSCs from healthy patients (Figure 2d), corresponding with an almost undetectable protein expression (Figure 2e). However, in BMMSCs from MGUS or MM patients, expression of PADI was greatly increased (Figure 2d and e): indeed mRNA expression was increased greater than 30-fold. Corresponding mRNA expression of other PADI family members was unchanged (Supplementary Figure 2). We therefore assessed the activity of PADI2 through its citrullination of a recently described target: histone H3R26cit(27). We found that this modification of histone H3 was significantly

increased in BMMSCs from MGUS and MM compared to healthy individuals (Figure 2e), where it was almost universally absent. In contrast, citrullination of other arginine residues in histone H3 that represent more specific PADI4 targets (R2, R8 and R17) were not upregulated to the same extent, suggesting that PADI2 activity, rather PADI4 was likely to be responsible for H3R26cit levels observed.

BMMSCs have been shown to play an important role in the support of malignant plasma cell survival, proliferation and resistance to chemotherapy(36). We therefore hypothesised that increased expression of PADI2 may alter the ability of the BMMSC to perform this function. We had previously noted that within the primary BMMSCs we isolated from MGUS and MM patients, some had relatively low expression of PADI2 while others were higher. We therefore selected two lines each of 'low' and 'high' expressers (Figure 2e, MGUS samples 2 and 5 [low] or 3 and 4 [high], Supplementary Table 2), and co-cultured these with JLN3 cells using a TransWell system for 24 hours before treatment with the clinically relevant chemotherapeutic agent, bortezomib. Although physically separate, the two cell lines could interact through metabolic or secreted factor interactions. We found that although co-culture with low PADI2-expressing BMMSCs had little effect on JLN3 cell viability after bortezomib treatment, high PADI2-expressing resulted in a significant protection, reducing the cell death induced by about 75% (Figure 3a). Interestingly, pre-incubating the high PADI2-expressing BMMSCs with the pan-PADI inhibitor CI-Amidine before co-culture with JLN3 cells led to a significant increase in bortezomib-induced apoptosis of the JLN3 cells (Figure 3b). These data overall suggested that at least part of the protection from chemotherapy-induced apoptosis elicited by BMMSCs was through a PADI2-mediated event. It had previously been shown that IL-6 production in the bone marrow microenvironment is important for the acquisition of resistance phenotypes by the plasma cells(20, 37, 38), with evidence for a role in bortezomib-induced resistance(39). We therefore investigated IL-6 expression by BMMSCs, and observed significant increased transcription of IL-6 mRNA (Figure 3c), which led to enhanced secretion into the medium from primary cells from MGUS and MM (Figure

3d). In addition, when mRNA expression of IL-6 was plotted against that of PADI2, we found that they were positively correlated (Figure 3e), providing further evidence for a mechanistic link between these two factors in MGUS and MM.

Using an immortalised, non-transformed BMMSC line (HS5), we assessed the effect of siRNA-mediated reduction in PADI2 expression (Figure 4a) on the expression of IL-6, as well as other factors expressed by BMMSCs known to play a role in MM pathogenesis: CXCL12 and cMET. We found that expression of all three pro-malignant factors was decreased when PADI2 expression was also reduced, or PADI activity was inhibited by Cl-Amidine (Figure 4b). Importantly, siRNA of PADI4 (Figure 4a) did not affect expression of any of these factors, showing that this effect was specifically through modulation of PADI2 expression (Figure 4b). Expression of another important factor in the pathogenesis of MM, vascular endothelial growth factor (VEGF), was not found to be modulated by PADI2 or PADI4 expression (Supplementary Figure 3). We directly tested the effect of knocking down or inhibiting PADI2 on IL-6 secretion into the medium of HS5 cells through siRNA or Cl-Amidine treatment, and found that IL-6 was reduced in both conditions, and not further reduced by combining both siRNA and inhibitor (Figure 4c), further supporting our findings that PADI2 is the main PADI family member that regulates IL-6 expression in BMMSCs. Finally, we over-expressed PADI2 and found that IL-6 mRNA expression was increased 10-fold (Figure 4d), whereas expression of an active-site mutant of PADI2 C647S(40) had no effect (Figure 4d). These data therefore provide direct mechanistic link between the expression of PADI2 and increased IL-6 production in BMMSCs from MGUS/MM patients.

It has previously been shown that PADI2 activity can citrullinate the R26 residue of histone H3 (H3R26cit), resulting in increased transcription of a number of genes(27). Our data also showed increased levels of this modification in BMMSCs from MGUS and MM (Figure 2e). We therefore hypothesised that the mechanism by which PADI2 activity could modulate transcription from the *IL-6* locus was through increasing citrullination of H3R26 in its

promoter. Primer pairs that covered the *IL-6* promoter region were designed (Figure 5a), and a chromatin immunoprecipitation experiment performed, in which after either siPADI2 or CI-Amidine treatment, antibodies against H3R26cit and trimethylated K4 of histone H3 (H3K4me3) were used to pull down chromatin associated with these modifications. H3K4me3, a modification associated with active areas of chromatin, was used as a positive control to determine whether changes in expression altered the overall activation state of the chromatin. We found that both CI-Amidine (Figure 5b) and siPADI2 (Figure 5d) decreased the enrichment of H3R26cit in the *IL-6* promoter region, the effects of which were particularly pronounced at and downstream of the transcription start site (TSS; Figure 5a). This correlated with a loss of the activating histone mark, H3K4me3 in the same conditions (CI-Amidine; Figure 5c, siPADI2; Figure 5e), indicating reduced activation of the *IL-6* promoter locus as a result of reduced PADI2 activity.

Our data therefore show that PADI2 expression correlates with *IL-6* expression in primary BMMSCs from patients with MGUS and MM (Figure 3) as well as citrullination of the H3R26 (Figure 2e) in the same cells. In addition, we have shown that PADI2 expression can directly increase *IL-6* expression (Figure 4) through citrullination of the R26 residue of histone H3 in the promoter region of the gene (Figure 5). Finally, we show that PADI2 expression and activity in BMMSCs can modulate malignant plasma cell resistance to the chemotherapeutic agent, bortezomib (Figure 3a&b, and Figure 6).

## Discussion

MM is an incurable disease that arises from the pre-malignant condition MGUS, present in the bone marrow of up to 7.5% of the elderly population(1, 41, 42). With increasing life expectancies and the resulting shift in the demographics of most developed countries, this disease represents a significant clinical challenge. Although it is now clear that the BM microenvironment is transformed in patients with MM, there are little data concerning the

nature of the MGUS microenvironment. We demonstrate here that BMMSCs from patients with both MGUS and MM have a transformed transcriptome compared to those from healthy individuals, in agreement with previous results(7). Our data, alongside those of others and our previous metabolomic study(35) highlight the significant similarities between the microenvironment of the BM in MGUS and MM, suggesting that transformation of the BM microenvironment is an early event in disease aetiology, raising the potential of interfering with this process in order to delay or prevent progression of patients with MGUS to MM. In addition, these data further highlight a need to identify those biological determinants in the BM that actually contribute to the progression of this disease: whether these are active drivers, or release of inhibitors of malignant progression.

Our data provide a mechanism by which IL-6 secretion is increased in BMMSCs of patients, which may contribute to treatment failure of bortezomib, a key therapeutic agent in MM treatment strategies. It is important to note, however, that anti-IL-6 therapy has not proven to be an efficacious agent in MM thus far, suggesting that targeting this signalling axis alone is likely to be insufficient to achieve clinical benefit(43). PADI2 may therefore represent a novel upstream target, as our data suggest that its activity increases expression of other central signalling networks between BMMSCs and myeloma cells, such as HGF-cMET and CXCL12-CXCR4 (Figure 4b). PADIs are a family of enzymes, of which PADI2 is becoming increasingly linked to a number of chronic diseases, including cancer(27, 44), rheumatoid arthritis(45), Alzheimer's disease(46) as well as autoimmune disease(47). Targets of the PADI enzymes include proteins with diverse functions such as extracellular matrix formation (e.g. vimentin and myelin) and chromatin structure (histone H3)(24). Importantly, as arginine citrullination is expected to be a relatively long-lived post-translational modification due to the absence of a characterised peptidylcitrullinase, these modifications may only be reversed through protein turnover. In the case of histone H3R26 citrullination within the *IL-6* promoter, this suggests that the chromatin unwinding and activation induced by this modification may only be reversed through proliferation or histone eviction. It is also highly

likely that a much larger number of pro-malignant transcripts are also modulated by the activity of PADI2. Indeed, a previous study of the effect of PADI2 on oestrogen receptor-mediated transcriptional regulation showed that it regulated over 200 transcripts in those conditions(27). Future work will focus on defining more of these targets in BMMSCs in order to determine the broader implications of PADI2 in the transformation of the healthy BM to that of MGUS/MM.

Therapeutic targeting of PADI2 may therefore represent a good (and early) therapeutic target in MGUS patients as well as those with MM, which may act by removing a significant proportion of the supportive signalling required by malignant plasma cells for survival and proliferation. Indeed, with the growing role for PADI2 in other chronic diseases, this enzyme may represent a novel therapeutic target in many pathological conditions.

### **Acknowledgements**

GMcN and DSW were supported by Bloodwise grant number 13039, SE and DBB by Cancer Research UK grant C1520/A9992 and KLE through Doctoral Training Grant from the Medical Research Council, reference MR/K501323/1. We wish to thank Professor Janet Lord for access to the Birmingham 1000 Elders cohort for peripheral blood samples from healthy aged individuals, and Dr. Kelly Chiang for advice on the chromatin immunoprecipitation analysis. We gratefully acknowledge the contribution to this study made by the University of Birmingham's Human Biomaterials Resource Centre which has been supported through Birmingham Science City - Experimental Medicine Network of Excellence project.

### **Authorship contributions**

GMcN, KLE, DSW, DBB, SE, WW and CCD performed experiments. AB, SA and GP obtained both patient consent and collected samples. PAHM, AF, SB, GP and DAT conceived, organised and managed the study and wrote the manuscript.

### Conflict of Interest

The authors declare no conflicts of interest

### References

1. Landgren O, Kyle RA, Pfeiffer RM, Katzmann JA, Caporaso NE, Hayes RB, et al. Monoclonal gammopathy of undetermined significance (MGUS) consistently precedes multiple myeloma: a prospective study. *Blood*. 2009;113(22):5412-7.
2. Chiecchio L, Dagrada GP, Ibrahim AH, Dachs Cabanas E, Protheroe RK, Stockley DM, et al. Timing of acquisition of deletion 13 in plasma cell dyscrasias is dependent on genetic context. *Haematologica*. 2009;94(12):1708-13.
3. Landgren O. Monoclonal gammopathy of undetermined significance and smoldering multiple myeloma: biological insights and early treatment strategies. *Hematology / the Education Program of the American Society of Hematology American Society of Hematology Education Program*. 2013;2013:478-87.
4. Hayashi T, Hideshima T, Akiyama M, Richardson P, Schlossman RL, Chauhan D, et al. Arsenic trioxide inhibits growth of human multiple myeloma cells in the bone marrow microenvironment. *Mol Cancer Ther*. 2002;1(10):851-60.
5. Mitsiades CS, McMillin DW, Klippel S, Hideshima T, Chauhan D, Richardson PG, et al. The role of the bone marrow microenvironment in the pathophysiology of myeloma and its significance in the development of more effective therapies. *Hematol Oncol Clin North Am*. 2007;21(6):1007-34, vii-viii.

6. Yasui H, Hideshima T, Richardson PG, Anderson KC. Novel therapeutic strategies targeting growth factor signalling cascades in multiple myeloma. *Br J Haematol*. 2006;132(4):385-97.
7. Corre J, Mahtouk K, Attal M, Gadelorge M, Huynh A, Fleury-Cappellesso S, et al. Bone marrow mesenchymal stem cells are abnormal in multiple myeloma. *Leukemia*. 2007;21(5):1079-88.
8. Garderet L, Mazurier C, Chapel A, Ernou I, Boutin L, Holy X, et al. Mesenchymal stem cell abnormalities in patients with multiple myeloma. *Leuk Lymphoma*. 2007;48(10):2032-41.
9. Wallace SR, Oken MM, Lunetta KL, Panoskaltis-Mortari A, Masellis AM. Abnormalities of bone marrow mesenchymal cells in multiple myeloma patients. *Cancer*. 2001;91(7):1219-30.
10. Zdzisinska B, Bojarska-Junak A, Dmoszynska A, Kandefer-Szerszen M. Abnormal cytokine production by bone marrow stromal cells of multiple myeloma patients in response to RPMI8226 myeloma cells. *Arch Immunol Ther Exp (Warsz)*. 2008;56(3):207-21.
11. Arnulf B, Lecourt S, Soulier J, Ternaux B, Lacassagne MN, Crinquette A, et al. Phenotypic and functional characterization of bone marrow mesenchymal stem cells derived from patients with multiple myeloma. *Leukemia*. 2007;21(1):158-63.
12. Garayoa M, Garcia JL, Santamaria C, Garcia-Gomez A, Blanco JF, Pandiella A, et al. Mesenchymal stem cells from multiple myeloma patients display distinct genomic profile as compared with those from normal donors. *Leukemia*. 2009;23(8):1515-27.
13. Hideshima T, Mitsiades C, Tonon G, Richardson PG, Anderson KC. Understanding multiple myeloma pathogenesis in the bone marrow to identify new therapeutic targets. *Nat Rev Cancer*. 2007;7(8):585-98.
14. Chauhan D, Uchiyama H, Akbarali Y, Urashima M, Yamamoto K, Libermann TA, et al. Multiple myeloma cell adhesion-induced interleukin-6 expression in bone marrow stromal cells involves activation of NF-kappa B. *Blood*. 1996;87(3):1104-12.

15. Hideshima T, Chauhan D, Hayashi T, Podar K, Akiyama M, Gupta D, et al. The biological sequelae of stromal cell-derived factor-1alpha in multiple myeloma. *Mol Cancer Ther.* 2002;1(7):539-44.
16. Podar K, Tai YT, Davies FE, Lentzsch S, Sattler M, Hideshima T, et al. Vascular endothelial growth factor triggers signaling cascades mediating multiple myeloma cell growth and migration. *Blood.* 2001;98(2):428-35.
17. Otsuki T, Yamada O, Yata K, Sakaguchi H, Kurebayashi J, Nakazawa N, et al. Expression of fibroblast growth factor and FGF-receptor family genes in human myeloma cells, including lines possessing t(4;14)(q16.3;q32. 3) and FGFR3 translocation. *Int J Oncol.* 1999;15(6):1205-12.
18. Sati HI, Greaves M, Apperley JF, Russell RG, Croucher PI. Expression of interleukin-1beta and tumour necrosis factor-alpha in plasma cells from patients with multiple myeloma. *Br J Haematol.* 1999;104(2):350-7.
19. Derksen PW, de Gorter DJ, Meijer HP, Bende RJ, van Dijk M, Lokhorst HM, et al. The hepatocyte growth factor/Met pathway controls proliferation and apoptosis in multiple myeloma. *Leukemia.* 2003;17(4):764-74.
20. Cheung WC, Van Ness B. Distinct IL-6 signal transduction leads to growth arrest and death in B cells or growth promotion and cell survival in myeloma cells. *Leukemia.* 2002;16(6):1182-8.
21. Dezorella N, Pevsner-Fischer M, Deutsch V, Kay S, Baron S, Stern R, et al. Mesenchymal stromal cells revert multiple myeloma cells to less differentiated phenotype by the combined activities of adhesive interactions and interleukin-6. *Exp Cell Res.* 2009;315(11):1904-13.
22. Wang S, Wang Y. Peptidylarginine deiminases in citrullination, gene regulation, health and pathogenesis. *Biochim Biophys Acta.* 2013;1829(10):1126-35.
23. Rus'd AA, Ikejiri Y, Ono H, Yonekawa T, Shiraiwa M, Kawada A, et al. Molecular cloning of cDNAs of mouse peptidylarginine deiminase type I, type III and type IV, and the expression pattern of type I in mouse. *Eur J Biochem.* 1999;259(3):660-9.

24. Vossenaar ER, Zendman AJ, van Venrooij WJ, Pruijn GJ. PAD, a growing family of citrullinating enzymes: genes, features and involvement in disease. *Bioessays*. 2003;25(11):1106-18.
25. Foulquier C, Sebbag M, Clavel C, Chapuy-Regaud S, Al Badine R, Mechin MC, et al. Peptidyl arginine deiminase type 2 (PAD-2) and PAD-4 but not PAD-1, PAD-3, and PAD-6 are expressed in rheumatoid arthritis synovium in close association with tissue inflammation. *Arthritis Rheum*. 2007;56(11):3541-53.
26. van Beers JJ, Zendman AJ, Raijmakers R, Stammen-Vogelzangs J, Pruijn GJ. Peptidylarginine deiminase expression and activity in PAD2 knock-out and PAD4-low mice. *Biochimie*. 2013;95(2):299-308.
27. Zhang X, Bolt M, Guertin MJ, Chen W, Zhang S, Cherrington BD, et al. Peptidylarginine deiminase 2-catalyzed histone H3 arginine 26 citrullination facilitates estrogen receptor alpha target gene activation. *Proc Natl Acad Sci U S A*. 2012;109(33):13331-6.
28. Cuthbert GL, Daujat S, Snowden AW, Erdjument-Bromage H, Hagiwara T, Yamada M, et al. Histone deimination antagonizes arginine methylation. *Cell*. 2004;118(5):545-53.
29. Wang Y, Wysocka J, Sayegh J, Lee YH, Perlin JR, Leonelli L, et al. Human PAD4 regulates histone arginine methylation levels via demethylimination. *Science*. 2004;306(5694):279-83.
30. Wettenhall JM, Smyth GK. limmaGUI: a graphical user interface for linear modeling of microarray data. *Bioinformatics*. 2004;20(18):3705-6.
31. Koch CM, Andrews RM, Flicek P, Dillon SC, Karaoz U, Clelland GK, et al. The landscape of histone modifications across 1% of the human genome in five human cell lines. *Genome Res*. 2007;17(6):691-707.
32. Qiang YW, Chen Y, Stephens O, Brown N, Chen B, Epstein J, et al. Myeloma-derived Dickkopf-1 disrupts Wnt-regulated osteoprotegerin and RANKL production by osteoblasts: a potential mechanism underlying osteolytic bone lesions in multiple myeloma. *Blood*. 2008;112(1):196-207.

33. Yaccoby S, Ling W, Zhan F, Walker R, Barlogie B, Shaughnessy JD, Jr. Antibody-based inhibition of DKK1 suppresses tumor-induced bone resorption and multiple myeloma growth in vivo. *Blood*. 2007;109(5):2106-11.
34. Tian E, Zhan F, Walker R, Rasmussen E, Ma Y, Barlogie B, et al. The role of the Wnt-signaling antagonist DKK1 in the development of osteolytic lesions in multiple myeloma. *N Engl J Med*. 2003;349(26):2483-94.
35. Ludwig C, Williams DS, Bartlett DB, Essex SJ, McNee G, Allwood JW, et al. Alterations in bone marrow metabolism are an early and consistent feature during the development of MGUS and multiple myeloma. *Blood Cancer J*. 2015;5:e359.
36. Bergfeld SA, Blavier L, DeClerck YA. Bone marrow-derived mesenchymal stromal cells promote survival and drug resistance in tumor cells. *Mol Cancer Ther*. 2014;13(4):962-75.
37. Lu Y, Zhang J, Dai J, Dehne LA, Mizokami A, Yao Z, et al. Osteoblasts induce prostate cancer proliferation and PSA expression through interleukin-6-mediated activation of the androgen receptor. *Clin Exp Metastasis*. 2004;21(5):399-408.
38. Bommert K, Bargou RC, Stuhmer T. Signalling and survival pathways in multiple myeloma. *Eur J Cancer*. 2006;42(11):1574-80.
39. Voorhees PM, Chen Q, Kuhn DJ, Small GW, Hunsucker SA, Strader JS, et al. Inhibition of interleukin-6 signaling with CNTO 328 enhances the activity of bortezomib in preclinical models of multiple myeloma. *Clin Cancer Res*. 2007;13(21):6469-78.
40. Dreyton CJ, Knuckley B, Jones JE, Lewallen DM, Thompson PR. Mechanistic studies of protein arginine deiminase 2: evidence for a substrate-assisted mechanism. *Biochemistry*. 2014;53(27):4426-33.
41. Cohen HJ, Crawford J, Rao MK, Pieper CF, Currie MS. Racial differences in the prevalence of monoclonal gammopathy in a community-based sample of the elderly. *Am J Med*. 1998;104(5):439-44.

42. Kyle RA, Beard CM, O'Fallon WM, Kurland LT. Incidence of multiple myeloma in Olmsted County, Minnesota: 1978 through 1990, with a review of the trend since 1945. *J Clin Oncol.* 1994;12(8):1577-83.
43. San-Miguel J, Blade J, Shpilberg O, Grosicki S, Maloisel F, Min CK, et al. Phase 2 randomized study of bortezomib-melphalan-prednisone with or without siltuximab (anti-IL-6) in multiple myeloma. *Blood.* 2014;123(26):4136-42.
44. McElwee JL, Mohanan S, Horibata S, Sams KL, Anguish LJ, McLean D, et al. PAD2 overexpression in transgenic mice promotes spontaneous skin neoplasia. *Cancer Res.* 2014;74(21):6306-17.
45. Vossenaar ER, Radstake TR, van der Heijden A, van Mansum MA, Dieteren C, de Rooij DJ, et al. Expression and activity of citrullinating peptidylarginine deiminase enzymes in monocytes and macrophages. *Ann Rheum Dis.* 2004;63(4):373-81.
46. Ishigami A, Masutomi H, Handa S, Nakamura M, Nakaya S, Uchida Y, et al. Mass spectrometric identification of citrullination sites and immunohistochemical detection of citrullinated glial fibrillary acidic protein in Alzheimer's disease brains. *J Neurosci Res.* 2015;93(11):1664-74.
47. Carrillo-Vico A, Leech MD, Anderton SM. Contribution of myelin autoantigen citrullination to T cell autoaggression in the central nervous system. *J Immunol.* 2010;184(6):2839-46.

**Figure Legends**

**Figure 1:** Heatmap of transcriptomic analysis from thirty BMMSC samples, 10 each from control, MGUS and MM patients shows that cells from patients with MGUS and MM cluster together, and are different from those isolated from healthy individuals. 74 genes were identified with a cut-off for gene expression change of >2.0 fold, and  $p < 0.001$ .

**Figure 2a:** Three of the top five upregulated transcripts that differed between control and 'disease' (MGUS/MM) BMMSCs identified from the transcriptomic analysis were the peptidyl arginine deiminase, PADI2 (**a**), filaggrin (**b**) and the urea transporter, SLC14A1 (**c**). **d:** PADI2 mRNA expression in BMMSCs from controls, MGUS and MM patients compared to beta-actin, analysed using Taqman, plotted on a logarithmic scale. Significant changes shown were calculated using Mann-Whitney tests. \*,  $p < 0.05$ , \*\*,  $p < 0.005$ , \*\*\*\*,  $p < 0.0001$ . **e:** BMMSCs derived from patients with MGUS and MM have greatly increased expression of PADI2 and citrullination of histone H3 on residue R26 (R26cit) compared to healthy controls. Citrullination of other arginine residues on histone H3 (R2,8,17) under the control of PADI4 are not similarly consistently increased. 'C<sub>L</sub>' and 'C<sub>H</sub>' indicate control samples (C<sub>L</sub>: low expressing, C<sub>H</sub>: high expressing) analysed on each blot in order for blots to be more easily compared.

**Figure 3a:** Expression of PADI2 protects plasma cells from chemotherapy-induced apoptosis. JJN3 cell apoptosis as a percentage of total cells, either untreated ('JJN3'), or 24 hours after treatment with 10 nM bortezomib ('+BTM'). When co-cultured with either a low PADI2-expressing ('PADI2 low') or high PADI2-expressing ('PADI2 High') BMMSCs across a Boyden chamber, JJN3 cells are partially protected from bortezomib-induced apoptosis, with extent of protection correlating with PADI2 expression. Two primary BMMSC lines were used per assay, each repeated  $n=3$ . Data were analysed by Kruskal-Wallis test ( $p < 0.0001$ ), with Dunn's multiple comparisons test to test for those values that were significantly different. Error bars show standard deviation. **b:** Inhibition of total PADI activity in the PADI2

High expressing lines using the pharmacological inhibitor, Cl-Amidine ('CL') significantly reduces acquired protection from bortezomib. Data were analysed using Mann-Whitney test, error bars show standard deviation. '\*\*\*';  $p=0.002$  **c**: IL-6 expression is significantly increased in BMMSCs derived from patients with MGUS and MM compared to controls. IL-6 mRNA expression was normalised to beta-actin. Significant changes shown between groups were calculated using Mann-Whitney tests. '\*\*\*\*';  $p<0.0001$ . Error bars are **d**: Bone marrow concentrations of IL-6 are also increased in patients with MGUS and MM. Mann-Whitney tests were again used to calculate significance of differences between groups. '\*\*\*';  $p=0.0005$ , '\*\*\*\*';  $p<0.0001$  **e**: Scatterplot of the expression of PADI2 against IL-6 as measured in BMMSCs from 38 patients with MM and MGUS shows that their expression is highly correlated ( $r^2 = 0.540$ , non-linear fit).

**Figure 4a:** Confirmation of knockdown by siPADI2 by two independent siRNA sequences.

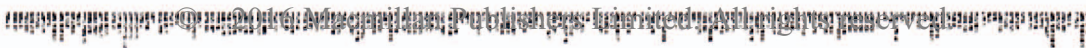
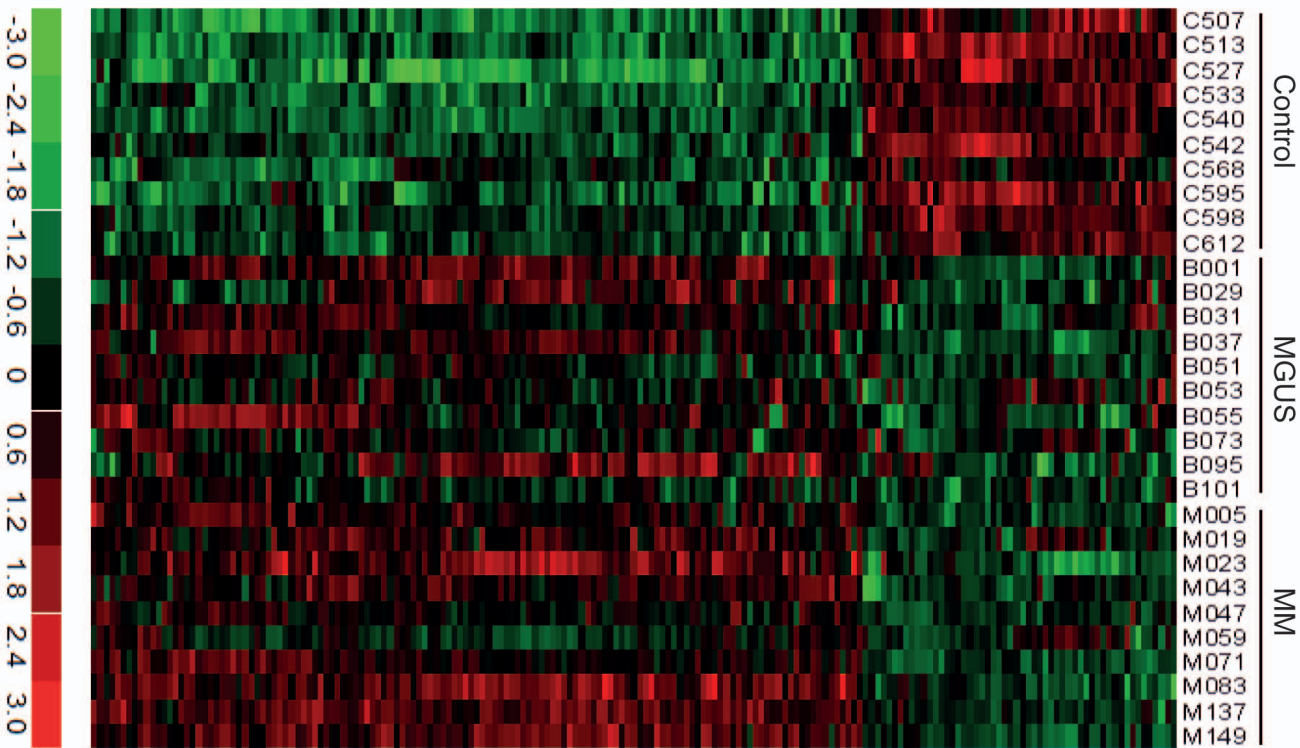
**b:** The expression of the BMMSC component of critical chemokine signalling axes in myeloma (IL-6, CXCL12 and cMET) is modulated by PADI2 expression in the immortalised BMMSC cell line, HS5. Expression of all three transcripts are reduced in response to reduction in PADI2 expression (siPADI2), or the addition of the pan-PADI inhibitor, Cl-Amidine (200  $\mu$ M, 72 hours). However, siPADI4 does not alter expression of any of the transcripts. **c:** IL-6 expression, as measured through its secretion into the tissue culture medium by the HS5 cell line, is reduced after treatment with Cl-Amidine and/or siPADI2. Data shown are mean of  $n=3 \pm$  standard deviation.  $p=0.039$ , unpaired student's t-test with Welch's correction. **d:** Over-expression of PADI2 increases IL-6 expression, whilst the catalytic mutant, C645S, does not increase expression over basal levels. Data shown are mean of  $n=3 \pm$  standard deviation.  $p=0.004$ , unpaired student's t-test with Welch's correction.

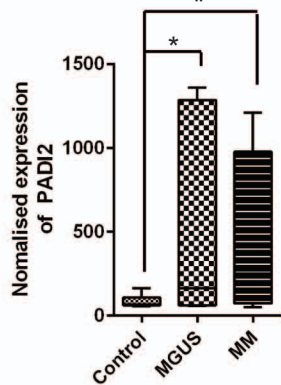
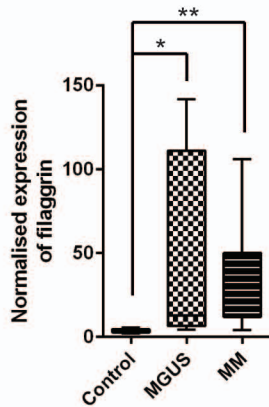
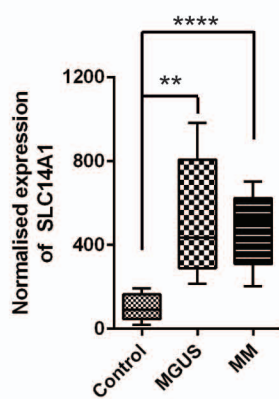
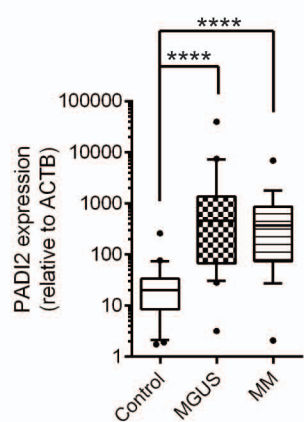
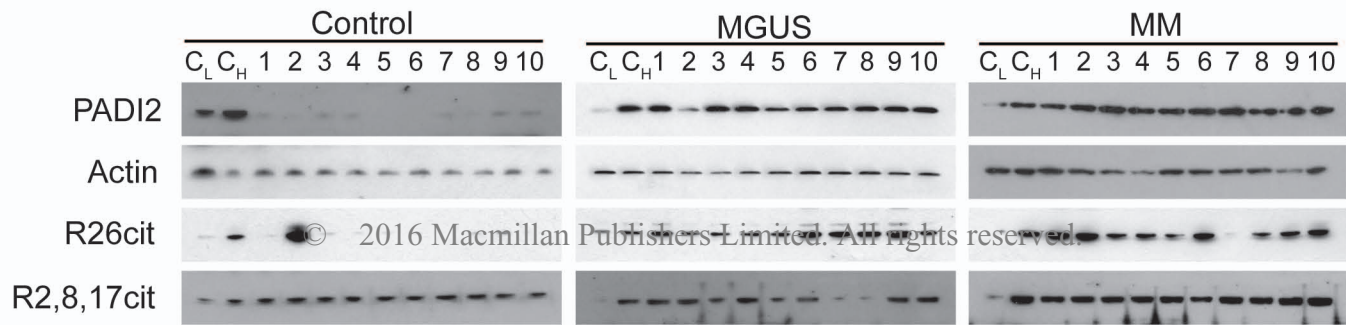
**Figure 5a:** Diagram showing the coverage of the *IL-6* promoter region by the primer pairs used in the chromatin immunoprecipitation analysis. Pull-down of chromatin associated with either citrullinated R26 (**b** and **d**) or trimethylated K4 (**c** and **e**) of histone H3, show that both

inhibition of PADI activity by Cl-Amidine (**b** and **c**) and reduction of PADI2 expression (through siRNA, **d** and **e**) reduce the enrichment of these marks on and downstream of the *IL-6* transcription start site, indicating that PADI2 activity is required for full activation of transcription from this locus.

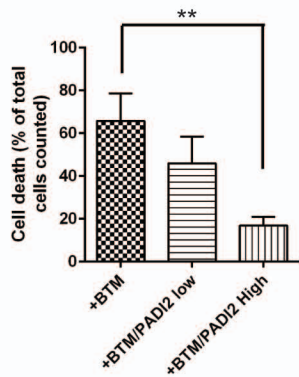
**Figure 6:** Model of how PADI2 activity in BMMSCs directly contributes to malignant plasma cell phenotype in patients with MGUS and MM. PADI2 citrullinates histone H3 at residue R26 within the promoter region of the *IL-6* gene, which increases its expression and secretion. IL-6 can then mediate its effects on other cells within the bone marrow, including the malignant plasma cells, which become more resistant to chemotherapeutic agents, such as Bortezomib.

Accepted manuscript

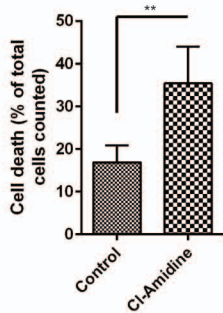


**a****b****c****d****e**

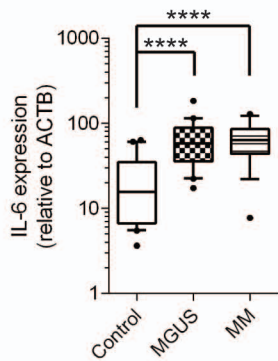
a



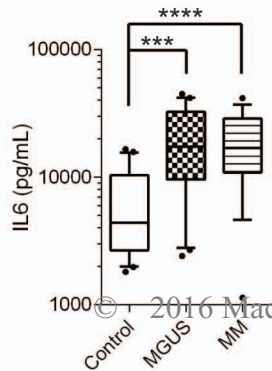
b



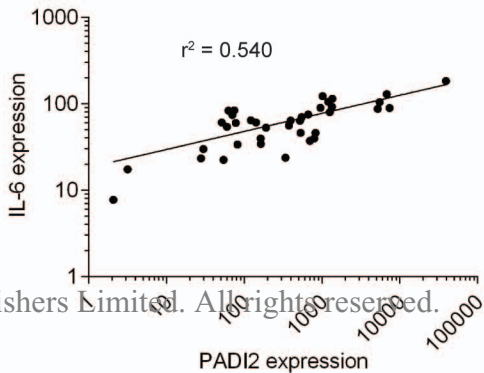
c



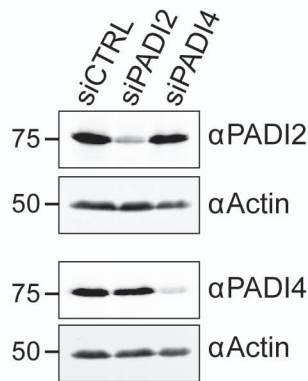
d



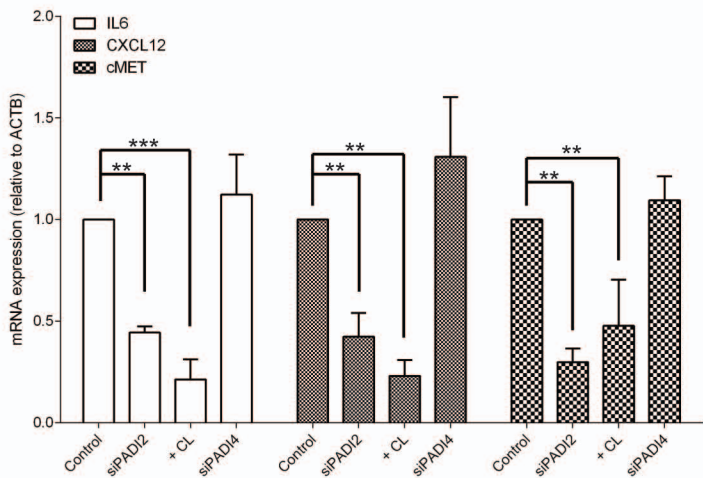
e



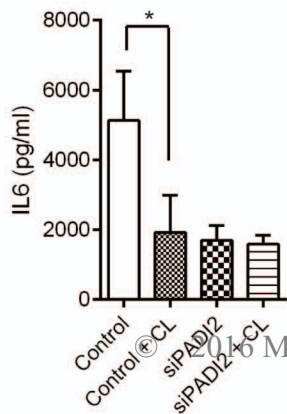
a



b



c



d

